

METRIC RADIO OBSERVATIONS AND RAY-TRACING ANALYSIS OF THE ONSET PHASE OF A SOLAR ERUPTIVE EVENT

C. KATHIRAVAN, R. RAMESH, AND K. R. SUBRAMANIAN

Indian Institute of Astrophysics, Bangalore 560-034, India; kathir@iiap.ernet.in,
ramesh@iiap.ernet.in, subra@iiap.ernet.in

Received 2001 December 6; accepted 2002 January 23; published 2002 February 5

ABSTRACT

We report metric radio observations and the results obtained using two-dimensional ray-tracing analysis of the solar corona close to the onset phase of the exceptionally bright prominence eruption and the associated massive coronal mass ejection (CME) of 1998 June 2. The average electron density of the observed radio enhancements at the location of the eruption was found to be ~ 17 times greater than the ambient medium. We also calculated their width along the line of sight, and the mean value is $\approx 160,000$ km. The radio estimate of the CME mass was about 4 times less than that of the white-light value.

Subject headings: solar-terrestrial relations — Sun: activity — Sun: corona — Sun: prominences —
Sun: radio radiation

1. INTRODUCTION

Most of the current observations of coronal mass ejections (CMEs) are from coronagraphs that detect them in Thomson-scattered sunlight above their occulting disks. The occulter of the coronagraph generally covers both the solar disk as well as the inner corona ($\leq 1.3 R_{\odot}$, R_{\odot} = solar radius = 6.96×10^5 km). Hence, the white-light observations have the inherent difficulty in providing information about the early evolution of CMEs. A study of the near-surface onset phase of a CME is considered to be very important since the basic physical state of a CME is completely determined at its initiation. Its subsequent development during the transit through the heliosphere is just an evolutionary process (Dere et al. 1997). In this respect, imaging observations at radio wavelengths play an important role since they do not have the limitation of an occulting disk and the CMEs can be detected early in their development via the thermal bremsstrahlung radiation they emit (Sheridan et al. 1978; Gopalswamy & Kundu 1992). Also, one can observe activity at any longitude similar to X-ray and EUV wavelengths. Again, the frontal structure of a CME has a large optical depth at meter wavelengths and can be readily observed (Bastian & Gary 1997; Gopalswamy 1999). In this Letter, we report one such observation close to the onset phase of a huge eruptive event from the solar atmosphere and the first successful modeling of the observed two-dimensional radio brightness distribution using the ray-tracing technique.

2. OBSERVATIONS

The radio data reported were obtained on 1998 June 2 with the low-frequency radioheliograph operating at the Gauribidanur Radio Observatory near Bangalore in India (see Ramesh et al. 1998 for details on the instrument). According to the CME catalog for the year 1998, the Large-Angle Spectroscopic Coronagraph (LASCO; Brueckner et al. 1995) on board the *Solar and Heliospheric Observatory (SOHO)* observed a massive CME on that day at around 08:08 UT (the time at which it was first noticed in the field of view of the LASCO C2 coronagraph). The above CME event was also accompanied by an exceptionally bright prominence eruption. Figure 1 shows a composite picture of the radioheliogram obtained at 109 MHz around 07:30 UT and the LASCO C2 image of the prominence

eruption/CME event obtained at 10:29:34 UT, on 1998 June 2. The central position angle (P.A., measured counterclockwise from the solar north) of the CME was 245° , and it had an angular span of 59° . The estimated speed (from a second-order fit) and acceleration of the CME in the plane of the sky were 1278 km s^{-1} and 45.2 m s^{-2} , respectively. The leading edge of the CME was observed at a projected height of $2 R_{\odot}$ around 07:40 UT in the field of view of the LASCO C1 coronagraph (Plunkett et al. 2000). This suggests that the extended, faint radio emission at the corresponding location in Figure 1 might be the counterpart of the former. The other bright white-light feature in the southeast quadrant is probably associated with the CME that took place around 03:00 UT at P.A. = 118° on that day. One can clearly notice its radio counterpart also at the corresponding location. We would like to point out here that it was possible for us to observe the faint radio signature associated with the above-mentioned two CME events mainly because of the following reasons: (1) they were not accompanied by any intense, nonthermal emission (as is usually the case with most of the CMEs) in our frequency range (Sol.-Geophys. Data 1998), and (2) the calibration scheme used for processing of the data obtained with the Gauribidanur radioheliograph (GRH) effectively makes use of the available redundancy in the length and orientation of the various baseline vectors and allows us to image sources with a dynamic range of ~ 20 dB (Ramesh, Subramanian, & Sastry 1999).

3. RAY-TRACING METHOD

In order to simulate the observed radio brightness distribution in Figure 1, we calculated the brightness distribution of the solar corona using various types of electron density and temperature distributions. We used a coronal model similar to that of Newkirk (1961) for a streamer in an otherwise spherically symmetric, homogeneous corona. The electron density at any point in the corona is given by

$$N_e(\rho) = N_0[1 + C_n \exp(-\beta^2)] \text{ cm}^{-3}, \quad (1)$$

where $N_0 = 4.2 \times 10^{4.32/\rho}$ (the spherically symmetric component of the background “quiet” Sun) and ρ is the radial distance from the center of the Sun. The constant C_n is the strength of the density enhancement/depletion, and β is the perpendicular

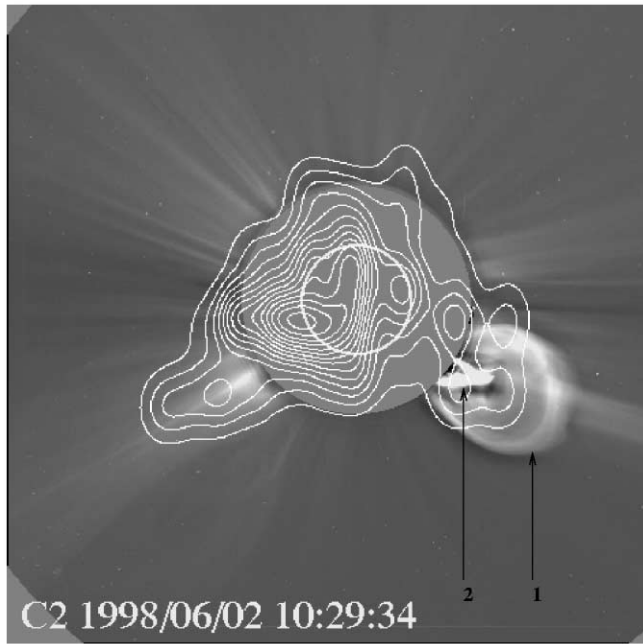


FIG. 1.—Composite picture showing the radioheliogram of the Sun at 109 MHz obtained with the GRH on 1998 June 2 at around 07:30 UT and the LASCO C2 image of the giant prominence eruption/CME observed on the same day. The peak brightness temperature in the radio map is $\sim 1.3 \times 10^6$ K. The contours are in intervals of 8.6×10^4 K. The open circle at the center is the solar limb. The outer circle is the occulter of the coronagraph. It extends approximately up to $2.2 R_{\odot}$ from the center of the Sun. The arrows labeled 1 and 2 indicate the CME and the prominence, respectively.

distance of the point from its axis. In the present case,

$$\beta^2 = \frac{(x - x_0)^2}{2\sigma_x^2} + \frac{(y - y_0)^2}{2\sigma_y^2} + \frac{(z - z_0)^2}{2\sigma_z^2}, \quad (2)$$

where σ_x , σ_y , σ_z and x_0 , y_0 , z_0 are the size (along the respective axes) and the location of the centroid of the density enhancement/depletion. Here x is toward the Earth (along the line of sight), and the (x, y) -plane contains the axis of the localized region; y and z represent the longitudinal and latitudinal directions on the Sun. All distances are in units of solar radius. For the localized regions, we used a model in which the density falls off as a Gaussian function along the x -, y -, and z -directions, from their centroid. To determine the brightness temperature (T_b) at some point in the solar corona, rays initially directed toward that point are traced (using the technique described in Newkirk 1961) from the Earth toward the Sun until the optical depth (τ) reaches a large value or the ray moves away from the Sun and is at least $5 R_{\odot}$ from the Sun. The brightness temperature (T_b) for any ray path is evaluated using the following integral:

$$T_b = \int_0^{\tau} T_e e^{-\tau} d\tau, \quad (3)$$

where T_e is the coronal electron temperature. The above procedure is repeated for different values of y and z , and the values are stored in a two-dimensional array. After trial and error, we were able to reproduce the observed brightness distribution by assuming a background corona of uniform brightness temperature ($T_e = 1.4 \times 10^6$ K) and a density profile equal to 0.35

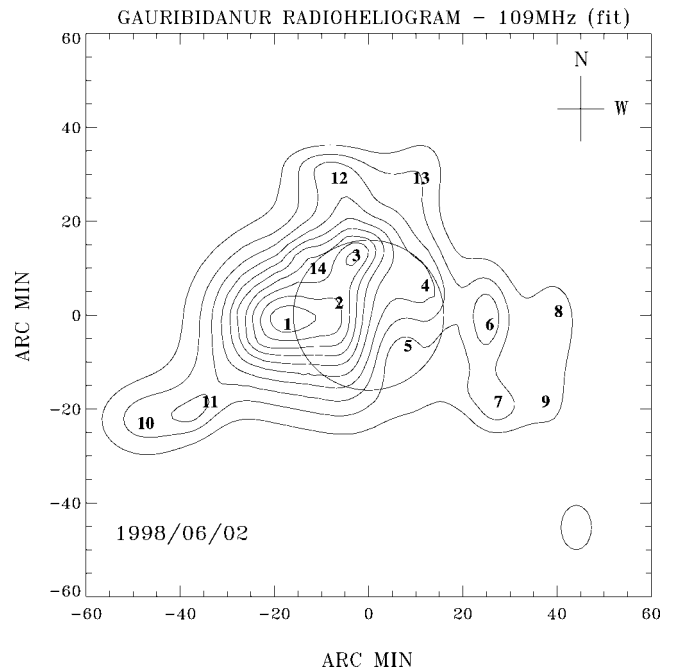


FIG. 2.—Radio brightness distribution of the Sun at 109 MHz obtained through ray-tracing calculations. The peak brightness temperature is $\sim 1.25 \times 10^6$ K. The contours are in intervals of 10^5 K. The instrument beam size is indicated at the bottom right-hand corner. The numbers 1–14 indicate the locations of the centroids of the discrete sources listed in Table 1.

times that given by equation (1). These values agree well with that reported recently by Fludra et al. (1999) for the quiet Sun. Figure 2 shows the brightness distribution obtained using the ray-tracing technique described above. There is a good correspondence with the observed radio brightness distribution in Figure 1. It is to be noted here that we have not included scattering (by small-scale density inhomogeneities in the solar corona) since their effects are more pronounced mainly at decimeter wavelengths (Aubier, Leblanc, & Boischoat 1971).

4. ANALYSIS AND RESULTS

Table 1 shows the parameters of the various localized sources used in the present calculations. They are consistent with those

TABLE 1
PARAMETERS OF THE DISCRETE SOURCES USED IN THE RAY-TRACING CALCULATIONS

Source	Location of the Centroid ^a	Size ^b (R_{\odot})	Density Factor C_n
S1	1.40, -1.10, -0.06	0.70, 0.77, 0.67	20
S2	1.40, -0.20, -0.04	0.77, 0.35, 0.71	8
S3	1.40, -0.02, -0.04	0.77, 0.32, 0.32	10
S4	1.60, 0.75, 0.40	0.32, 0.27, 0.45	10
S5	1.23, 0.46, -0.46	0.39, 0.19, 0.32	-3
S6	1.50, 1.70, -0.06	0.20, 0.22, 0.64	10
S7	1.70, 1.72, -1.22	0.22, 0.29, 0.29	17
S8	1.70, 2.48, -0.03	0.26, 0.29, 0.50	20
S9	1.70, 2.44, -1.22	0.22, 0.29, 0.50	20
S10	1.70, -2.10, -1.30	0.22, 0.22, 0.22	15
S11	1.70, -2.86, -1.36	0.55, 0.53, 0.45	30
S12	1.70, -0.46, 1.95	0.50, 0.50, 0.27	12
S13	1.70, 0.80, 2.00	0.39, 0.32, 0.39	9
S14	1.50, -0.80, 0.90	0.15, 0.08, 0.08	25

^a In x -, y -, and z -coordinates and in units of solar radius from the center of the Sun.

^b Along the x -, y -, and z -axes.

used for modeling of discrete thermal sources at meter-decameter wavelengths (Schmahl, Gopalswamy, & Kundu 1994). The sources S6–S9 correspond to the observed enhancement at the location of the CME in the southwest quadrant in Figure 1, and their average electron density is $\approx 2.65 \times 10^7 \text{ cm}^{-3}$. This is about 17 times greater than the ambient density at $2.8 R_{\odot}$, the mean radial distance of the above sources. A similar value had been reported earlier by Stewart, Hansen, & Sheridan (1978) for the discrete radio sources observed by them in association with a solar eruptive event. Also, it is consistent with that reported earlier for CME events observed with *SOHO* (Akmal et al. 2001; Ciaravella et al. 2001). Assuming that the coronal plasma is a fully ionized gas of normal solar composition (90% hydrogen and 10% helium by number), one finds that each electron is associated with approximately 2×10^{-24} g of material. Therefore, the mass is given by

$$M = 2 \times 10^{-24} N_e V \text{ g}, \quad (4)$$

where V is the volume of the observed enhancement. Substituting for sources S6–S9 individually in equation (4), we get their total mass as 2.02×10^{15} g. This is less than that estimated using LASCOS observations of the same event, by about a factor of 4 (Vourlidas et al. 2000). It must be pointed out that the mass estimate by radio observations in the present case is closer to the Sun and is at an earlier time compared to the mass estimate by white-light observations. Gopalswamy et al. (1996) had reported a similar increase in the frontal mass of a CME over a distance of only $1 R_{\odot}$. They suggested that material from the eruptive prominence may also take coronal-like properties and contribute to the mass increase in the frontal structure.

5. CONCLUSIONS

We have estimated the electron density, volume, and mass of a CME by performing a ray-tracing analysis of the metric radio observations of the event. The estimated electron density is consistent with that reported earlier from the *SOHO* Ultraviolet Coronagraph Spectrometer observations of similar events and is about 17 times greater than the ambient density. A knowledge of the width of the structure along the line of sight enabled us to calculate its volume, and hence the mass, in a straightforward manner. The estimated value of the mass is a factor of 4 less than the value reported using *SOHO/LASCO* white-light observations of the same event. The ray-tracing method would be useful in studying the characteristics of the radio-emitting structures associated with the onset phase of the eruptive solar activity, in an independent manner.

We thank Ch. V. Sastry for many useful discussions on the ray-tracing calculations. The *SOHO/LASCO* image presented in this Letter is due to the kind courtesy of Simon Plunkett. The comments of the referee (N. Gopalswamy) enabled us to bring out the results in a more clear fashion. We thank the staff of the Gauribidanur Radio Observatory for their help in data collection and maintenance of the antenna and receiver systems. The *SOHO* data are produced by a consortium of the Naval Research Laboratory (US), Max-Planck-Institut für Aeronomie (Germany), Laboratoire d'Astronomie (France), and the University of Birmingham (UK). *SOHO* is a project of international cooperation between ESA and NASA. The CME catalog is generated and maintained by the Center for Solar Physics and Space Weather, the Catholic University of America, in cooperation with the Naval Research Laboratory and NASA.

REFERENCES

- Akmal, A., Raymond, J. C., Vourlidas, A., Thompson, B., Ciaravella, A., Ko, Y.-K., Uzzo, M., & Wu, R. 2001, *ApJ*, 553, 922
 Aubier, M., Leblanc, Y., & Boischoat, A. 1971, *A&A*, 12, 435
 Bastian, T. S., & Gary, D. E. 1997, *J. Geophys. Res.*, 102, 14,031
 Brueckner, G. E., et al. 1995, *Sol. Phys.*, 162, 357
 Ciaravella, A., Raymond, J. C., Reale, F., Strachan, L., & Peres, G. 2001, *ApJ*, 557, 351
 Dere, K. P., et al. 1997, *Sol. Phys.*, 175, 601
 Fludra, A., del Zanna, G., Alexander, D., & Bromage, B. J. I. 1999, *J. Geophys. Res.*, 104, 9709
 Gopalswamy, N. 1999, in *Proc. Nobeyama Symp. 1998 on Solar Physics with Radio Observations*, ed. T. S. Bastian, N. Gopalswamy, & K. Shibasaki (NRO Rep. 479; Nagano: NRO), 141
 Gopalswamy, N., & Kundu, M. R. 1992, *ApJ*, 390, L37
 Gopalswamy, N., Kundu, M. R., Hanaoka, Y., Enome, S., Lemen, J. R., & Akioka, M. 1996, *NewA*, 1, 207
 Newkirk, G., Jr. 1961, *ApJ*, 133, 983
 Plunkett, S. P., et al. 2000, *Sol. Phys.*, 194, 371
 Ramesh, R., Subramanian, K. R., & Sastry, Ch. V. 1999, *A&AS*, 139, 179
 Ramesh, R., Subramanian, K. R., Sundararajan, M. S., & Sastry, Ch. V. 1998, *Sol. Phys.*, 181, 439
 Schmahl, E. J., Gopalswamy, N., & Kundu, M. R. 1994, *Sol. Phys.*, 150, 325
 Sheridan, K. V., Jackson, B. V., McLearn, D. J., & Dulk, G. A. 1978, *Proc. Astron. Soc. Australia*, 3, 249
Sol.-Geophys. Data. 1998, 648, Part I
 Stewart, R. T., Hansen, R. T., & Sheridan, K. V. 1978, in *IAU Colloq. 40, Physics of Solar Prominences*, ed. E. Jensen, P. Maltby, & F. Q. Orrall (Oslo: Univ. Oslo/Inst. Theor. Astrophys.), 315
 Vourlidas, A., Subramanian, P., Dere, K. P., & Howard, R. A. 2000, *ApJ*, 534, 456